Studies of Protein–Protein Association between Yeast Cytochrome *c* Peroxidase and Yeast Iso-1 Ferricytochrome *c* by Hydrogen–Deuterium Exchange Labeling and Proton NMR Spectroscopy†

Qian Yi,‡ James E. Erman,§ and James D. Satterlee*,‖

Department of Biochemistry and Biophysics and Department of Chemistry, Washington State University, Pullman, Washington 99164-4630, and Department of Chemistry, Northern Illinois University, DeKalb, Illinois 60115

Received March 7, 1994; Revised Manuscript Received June 28, 1994®

ABSTRACT: Hydrogen–deuterium (H–D) exchange labeling and proton NMR have been applied to study the protein–protein association between cytochrome *c* peroxidase (CcP) and yeast iso-1 ferricytochrome *c*. Specifically, the exchange behavior of individual backbone amide protons of yeast iso-1 ferricytochrome *c* in both CcP-bound (i.e., complexed) and free (i.e., never in the complex) forms has been investigated and used in an attempt to map the binding site of CcP on yeast iso-1 ferricytochrome *c* when the noncovalent complex was formed in very low salt solution. The exchange rates of certain amino acid amide protons were significantly slowed down, by up to 40-fold, in the complex compared to the free form. The protected regions on iso-1 ferricytochrome *c* include parts of the 10's helix and the 70's helix surrounding the cytochrome *c* heme solvent-exposed edge (the so-called "front side" of iso-1 cytochrome *c*). These regions are very similar to the cytochrome *c* peroxidase binding interface on iso-1 ferricytochrome *c* that has been defined by X-ray crystallographic data. This further supports the direct involvement of the front side of iso-1 cytochrome *c* in binding with cytochrome *c* peroxidase. The results from our H–D exchange experiments also indicated that the amide proton exchange rates of Trp59, Asp60, and part of the 90's helix, all of which are located on the opposite side (the "back" side) of ferricytochrome *c* from the heme solvent-exposed edge, are also retarded upon complex formation.

Long-range electron transfer between redox proteins is very important in many biological processes, such as photosynthesis and respiration. Among all the biological redox partners, one of the most notable and most extensively studied protein redox pairs is cytochrome *c* (cyt *c*)[1] and cytochrome *c* peroxidase (CcP, EC 1.1.11.5) from baker's yeast. CcP catalyzes the two-electron reduction of hydrogen peroxide to water utilizing two reducing equivalents from ferrocytochrome *c* (Bosshard et al., 1991; Poulos & Kraut, 1980; Poulos & Finzel, 1984). Since CcP can spontaneously form a noncovalent complex with cyt *c* (Mochan, 1970) in solution at low ionic strength, it has been inferred that the interprotein electron-transfer steps involved in CcP catalysis occur via cyt *c* association with CcP.

A noncovalent complex between CcP and horse cytochrome *c* was first suggested from analysis of saturation kinetics (Chance, 1950; Nicholls, 1964; Yonetani & Ray, 1966), and it has stimulated many studies on this type of complex. For example, CcP/cyt *c* binding has been characterized by sedimentation velocity and gel filtration (Nicholls & Mochan, 1971; Margoliash et al., 1976; Kang et al., 1977), absorption spectroscopy (Erman & Vitello, 1980), fluorescence quenching (Leonard & Yonetani, 1973; Kornblatt & English, 1986; Vitello & Erman, 1987; McLendon et al., 1993), chemical cross-linking (Waldmeyer & Bosshard, 1985; Moench et al., 1992, 1993), and transient absorption spectroscopy (Stemp & Hoffman, 1993). Also, electron-transfer kinetic studies have been carried out for several CcP/cyt *c* complexes. These include primarily horse and yeast cytochrome *c* (isozyme 1 is the most common) (Ho et al., 1983; Hazzard et al., 1987, 1988a,b; Geren et al., 1991; Hahm et al., 1992). Finally, the structural consequences of CcP/cyt *c* complex formation have also been investigated both hypothetically, by molecular modeling (Poulos & Kraut, 1980) and Brownian dynamics simulation (Northrup et al., 1988, 1992), and experimentally, by NMR spectroscopy (Gupta & Yonetani, 1973; Satterlee et al., 1987; Moench et al., 1992; Yi et al., 1992, 1993a, 1994) and X-ray crystallography (Pelletier & Kraut, 1992). In most of these studies, a high-affinity 1:1 complex stoichiometry has been indicated and used for studying the association of CcP and cytochrome *c*, although evidence for the existence of a 1:2 (CcP/cyt *c*) complex has been presented (Kang et al., 1977; Stemp & Hoffman, 1993; Zhou & Hoffman, 1993).

Many of these previous studies have utilized various sources of cytochrome *c*, primarily horse, tuna, and yeast iso-1 cytochrome *c*, although only yeast iso-1 cytochrome *c* is the natural redox partner of CcP. Growing experimental evidence indicates that there is a high degree of species specificity associated with these complexes. The uniqueness of the CcP/yeast iso-1 cytochrome *c* complex has made it attractive for

† This work has been supported by a grant from the National Institutes of Health (GM45986 to J.D.S.) and by a grant from the National Science Foundation (MCB9121414 to J.E.E.). We appreciate this support and the support of the WSU NMR Center derived from the Battelle Pacific Northwest Laboratories and the NIH (Grant RR061401).

* Author to whom correspondence should be sent: telephone, 509-335-8620; Fax, 509-335-8867; Internet, hemeteam@cosy.chem.wsu.edu.

‡ Department of Biochemistry and Biophysics, Washington State University.

§ Department of Chemistry, Northern Illinois University.

‖ Department of Chemistry, Washington State University.

® Abstract published in *Advance ACS Abstracts,* September 1, 1994.

[1] Abbreviations: CcP, cytochrome *c* peroxidase (ferrocytochrome *c*:H_2O_2 oxidoreductase, 1.11.1.5); COSY, correlated spectroscopy; cyt *c*, cytochrome *c*; CcP/cyt *c*, the noncovalent complex formed between CcP and cytochrome *c*; DEAE-Sepharose, diethylaminoethyl-Sepharose; DQF-COSY, double-quantum-filtered correlated spectroscopy; H-bond, hydrogen bond; H–D exchange, hydrogen–deuterium exchange; MCOSY, magnitude correlated spectroscopy; NOESY, nuclear Overhauser effect spectroscopy; TOCSY, total correlated spectroscopy.

0006-2960/94/0433-12032$04.50/0

biological electron-transfer studies since understanding details of this physiological redox complex may provide essential insights as to how cytochrome c interacts with its other redox partners in photosynthesis and respiration.

The recent X-ray structures of the cocrystallized CcP/horse cyt c and CcP/yeast iso-1 cyt c complexes (Pelletier & Kraut, 1992) have attracted great attention and provided solid structural insights into the association of these two types of proteins. The published structures were of the high-affinity 1:1 stoichiometric complexes. In the case of the CcP/yeast iso-1 cyt c complex, a structural comparison revealed no significant conformational change for either CcP or cytochrome c. The limited solution NMR data on this complex (Moench et al., 1992; Yi et al., 1992, 1993a) are generally consistent with the crystallographic result. However, several significant complex-induced proton chemical shift changes for both ferricytchrome c and cyanide-ligated CcP are difficult to rationalize from the crystal structure. Some of those perturbed resonances are buried inside each of the proteins, and in the case of iso-1 cytochrome c they even occur in a region on iso-1 cyt c that is not directly involved in the binding interface that was defined by the crystal structure. This suggests that in solution the effect of complex formation is transmitted to parts of both proteins remote from the binding site, most likely via subtle structural changes, which were not detected in the crystal structures. Therefore, further investigation of the CcP/yeast iso-1 ferricyt c interaction interface seems necessary for further understanding the protein–protein association involved in forming these types of redox complexes.

Here we have used the hydrogen–deuterium (H–D) exchange labeling technique combined with two-dimensional NMR spectroscopy in an attempt to map the CcP binding site on the yeast iso-1 ferricyt c surface. The technique was pioneered by Englander and Roder and has been successfully used for determining the interface of several antibody/horse cyt c complexes (Paterson et al., 1990; Mayne et al., 1992). While this paper was in review, a report from this group appeared concerning experiments similar to those presented here, but for the CcP/horse ferricyt c complex (Jeng et al., 1994). For the CcP/yeast iso-1 ferricyt c complex, we have found that the H–D exchange rates of certain amide protons of yeast iso-1 ferricyt c were significantly retarded due to the CcP binding in low salt solution. Protection factors as high as ~40-fold were found, and the pattern of protection has been used to further study the structure of the complex in solution.

MATERIALS AND METHODS

Yeast cytochrome c peroxidase was isolated and purified as previously described (Erman & Vitello, 1980; Vitello et al., 1990). Yeast iso-1 cytochrome c (Sigma), which contains about 50% of the reduced form, was completely oxidized to the ferric form by $K_3Fe(CN)_6$ (Baker Analyzed). Excess $K_3Fe(CN)_6$ was removed by passing the ferricyt c through a Dowex 1-X8 (Bio-Rad) column prior to use. Protein concentrations were measured by visible spectroscopy using extinction coefficients of 106 mM^{-1} cm^{-1} at 409 nm for ferricyt c and 93 mM^{-1} cm^{-1} at 408 nm for CcP. The NMR experiments for determining the complex-induced proton chemical shift changes in the CcP/yeast iso-1 ferricyt c complex were obtained under the same experimental condition as reported in previous studies (Yi et al., 1992 1993a). In particular, the proton resonance shifts reported in Table 4 were obtained at a calibrated probe temperature of 20 °C.

Proton Resonance Assignments for Yeast Iso-1 Ferrocyt c. Yeast iso-1 ferrocyt c NMR samples for proton assignment experiments were prepared in 50 mM potassium phosphate/90% H_2O/10% D_2O buffer, pH 5.2. The pH was measured with a calibrated Fisher combination electrode and Accumet 925 (Fisher) meter. In D_2O solutions pH′ represents the meter reading without correction for the isotope effect. For these assignments, NMR data were collected at 25 °C on a Varian VXR500S spectrometer operating at the nominal proton frequency of 500 MHz. The following two-dimensional experiments were utilized to make proton assignments: magnitude correlated spectroscopy (MCOSY) (Bax et al., 1981; Martin & Zektzer, 1988), double-quantum-filtered COSY (Piatini et al., 1982), nuclear Overhauser effect spectroscopy (NOESY) (Kumar et al., 1981; States et al., 1982), and total correlation spectroscopy (TOCSY) (Otting & Wuthrich, 1987). All spectra were collected with a 8688-Hz spectral width, 2048 hypercomplex data points in the f_2 dimension, 512 t_1 increments, and 128 scans per block. All phase-sensitive spectra were acquired using the hypercomplex acquisition method of States et al. (1982). For NOESY experiments, 100- and 133-ms mixing time spectra were employed. For TOCSY experiments, mixing times of 40 and 60 ms were used. All two-dimensional data were processed with sine-bell apodization constants of 0.023–0.051 s. The H_2O resonance (4.70 ppm) was employed as an internal chemical shift reference, and residual H_2O intensity was suppressed by presaturation for 1 s during the recovery period.

Hydrogen–Deuterium Exchange Experiment. The H–D exchange reaction was carried out as follows. CcP and yeast iso-1 ferricyt c were mixed at a 1:1 mole ratio in a 10 mM KNO_3 solution, pH 6.5, in order to form the noncovalent complex. This solution was chosen to be consistent with earlier NMR studies from our laboratory (Moench et al., 1992; Yi et al., 1992, 1993a, 1994). An approximately 15% mole excess of CcP over yeast iso-1 ferricyt c was used to ensure that the ferricyt c was fully bound. The H–D reaction was initiated by passing the complex, which was formed in H_2O solution, through a Sephadex G-25 (Sigma) spinning gel filtration column (Jeng & Englander, 1992), which was preequilibrated with 10 mM KNO_3/D_2O solution, pH′ 6.5. Next, the sample was incubated at 23 °C for various time intervals ranging from 30 min to 96 h. During the incubation, each labile –NH proton in ferricyt c exchanged to –ND at its own characteristic rate. After the H–D exchange time period, each sample was cooled to 5 °C and the pH′ of the sample solution was lowered to 5.0 by adding dilute DCl. The low temperature and low pH is expected to severely retard further H–D exchange (Paterson et al., 1990).

The deuterium-labeled iso-1 ferricyt c was reisolated from CcP by applying the complex sample to a small fast-flow DEAE-Sepharose (Sigma) column preequilibrated with 10 mM phosphate/D_2O buffer at pH′ 5.0. Yeast iso-1 ferricyt c was eluted in 10 mM phosphate/D_2O buffer and subsequently reduced to the ferrous form with sodium dithionite (MCB). The reduced iso-1 cyt c was further concentrated and exchanged into 50 mM phosphate/D_2O buffer at pH′ 5.0 by centrifugal ultrafiltration with a YM3 membrane (Amicon) at 5 °C. The final concentration of iso-1 ferrocyt c was between 2 and 3 mM although the precise concentration is not important to these experiments. At this point, the sample was ready for NMR analysis. Free yeast iso-1 ferricyt c was run through the above procedures in parallel with each complex sample.

NMR Analysis for H–D Exchange. To quantitate the exchange reactions, two-dimensional proton magnitude COSY (MCOSY) spectra were collected on a Varian VXR500S spectrometer at 25 °C. For each spectrum, 400 t_1 increments

Table 1: Proton Assignments of Wild-Type Yeast Iso-1 Ferrocytochrome *c*[a]

residue	type[b]	amide	α	β	others	residue	type[b]	amide	α	β	others
Phe(−3)	f	8.72	4.39	2.66	δ 7.10, ε 7.38, ζ 7.21	Ala51	f	7.70	3.88	1.28	
Lys(−2)	f	6.58	3.83	1.18, 1.42	γ 1.30	Asn52	f	8.24	4.06		
Ala(−1)	f	7.75	3.66	1.28		Ile53	f	7.63	3.30	1.79	
Gly1	f	8.24	4.36			Lys54	f	9.10	3.83	1.75	
Ser2	f	9.51	4.82			Lys55	f	7.51	3.78	1.80	
Ala3	f	9.30	4.10	1.50		Asn56	f	6.99	4.29	2.95	
Lys4		no assignment				Val57	f	7.35	3.61	0.95	γ −0.32, γ 0.40
Lys5	f	7.77	4.16	1.76, 2.00	γ 0.87, γ 0.78	Leu58	f	8.28	3.70	1.74	γ 0.95, δ 0.22, δ 0.60
Gly6	f	8.81	4.20, 3.65			Trp59	m	7.98	4.98	3.70	
Ala7	f	8.07	2.40	1.15		Asp60	s	9.45	4.89	2.71, 2.84	
Thr8	f	7.24				Glu61		no assignment			
Leu9	f	7.98	4.08	2.21, 1.35	γ 1.75, δ 1.12, δ 0.92	Asn62	f	8.22			
Phe10	m	8.83	3.96	2.87	δ 6.20, ε 6.70, ζ 7.10	Asn63	f	9.54	4.46	3.38, 3.57	
Lys11	f	8.25				Met64	f	8.95			
Thr12	f	7.96	4.31	1.31		Ser65	s	7.80	3.89	3.66	
Arg13	m	8.59	5.10	2.84, 2.54	γ 2.18	Glu66	f	7.79	3.75	1.72, 1.35	
Cys14	m	8.00	5.23	1.00, 1.81		Tyr67	f	8.39			
Leu15	f	7.22				Leu68	s	8.30	3.00	1.69	γ 1.99, δ 0.11, δ 1.02
Gln16	f	8.82				Thr69	s	7.31	3.80	4.08	γ 1.01
Cys17	m	6.96	4.20	0.50, 1.50		Asn70	f	6.19	4.16	2.68, 2.83	
His18	s	6.51	3.54	0.79, 0.36	δ 0.02, ε 0.68	Pro71		no assignment			
Thr19	s	7.12	4.58			Tml72	f	7.70	3.74	1.71, 1.52	
Val20	m	7.50	3.87	1.78	γ −0.13, γ 0.30	Lys73	m	6.94	3.93	1.68, 1.57	γ 1.36, δ 3.81
Glu21	f	8.83	3.99			Tyr74	m	7.30	4.18	3.19, 3.06	
Lys22	f	8.67	3.14			Ile75	m	8.27	4.01	2.12	γ 0.54
Gly23	f	9.25	3.79, 3.49			Pro76		no assignment			
Gly24	f	7.85	3.96, 3.10			Gly77	f	8.60	3.51, 4.11		
Pro25		no assignment				Thr78	f	8.22	4.50	4.18	γ 0.75
His26	f	8.36	4.33			Lys79	f	8.75			
Lys27	f	7.67	4.27			Met80	f	6.99	3.00	−0.19, −2.40	γ −3.78, γ −1.80
Val28	f	7.02	3.88	2.00	γ 1.72, γ 1.22	Ala81	f	8.12	3.94	1.30	
Gly29	m	7.69	3.60			Phe82	f	6.20	4.35	1.95, 0.50	
Pro30		no assignment				Gly83	f	9.64			
Asn31		no assignment				Gly84		no assignment			
Leu32	f	7.80	3.93	1.10, 1.28	γ 0.29, δ −0.70, δ −0.90	Leu85		no assignment			
His33	f	7.50	3.76	2.85, 2.98		Lys86	f	8.40	3.90	1.80	
Gly34		no assignment				Lys87	f	8.90			
Ile35	s	7.17	3.60	1.56	γ 0.15, γ 0.85, γ 1.38	Glu88	f	9.00			
Phe36	f	7.95	4.23	3.88, 2.67	δ 7.19, ε 6.80, ζ 7.00	Lys89	f	8.72	3.93	1.69	
Gly37	f	8.79				Asp90	f	6.45	4.30	2.94, 2.67	
Arg38	f	8.08	4.80			Arg91	f	7.52	3.83	2.21, 1.99	δ 1.33
His39	f	7.91	5.58	2.75, 2.80		Asn92	f	8.68			
Ser40	f	8.71	4.75			Asp93		no assignment			
Gly41	f	8.69				Leu94	m	8.56	4.28	2.15	
Gln42	f	8.15	4.55	1.80	γ 2.40, γ 2.01	Ile95	s	9.27	3.67	2.11	γ 0.56
Ala43	f	8.66	4.31	1.32		Thr96	s	8.22	3.88	4.44	γ 1.20
Glu44	f	8.76	4.15	1.99, 2.28		Tyr97	s	7.84	4.15	3.20, 3.62	
Gly45	f	9.15	3.74	4.32		Leu98	s	9.19	3.43	1.65, 2.07	γ 1.95, δ 0.98, δ 0.70
Tyr46	f	7.15	4.10	1.09, 2.19		Lys99	s	8.58	3.39	1.35, 1.47	
Ser47	f	6.93	4.48	3.41, 3.62		Lys100	m	6.65	4.14	1.40, 1.80	γ 2.10
Tyr48	f	8.21	5.10	2.85		Ala101	f	8.42	3.82	0.51	
Thr49	f	10.23	4.41	4.71	γ 1.84	Cys102	f	7.73	4.03	3.75	
Asp50	f	8.66	4.43	2.54		Glu103	f	6.88	3.85	2.00, 2.28	γ 2.40

[a] Shifts are reported at 25 °C, pH 5.2, in 50 mM phosphate buffer, internally referenced to residual H_2O at 4.70 ppm. [b] Each amino acid is classified as fast (f), medium (m), or slow (s) depending upon the amide proton exchange rate in iso-1 ferricytochrome *c* as described in the text.

of 2048 hypercomplex data points over a 9000-Hz spectral width were collected with solvent presaturation during the relaxation delay. Each spectrum was processed with a sine-bell apodization constant of 0.023 s in both dimensions. For each H–D exchange time point, NH–Cα H cross-peak volumes of the slowly exchanging NH's were measured and normalized against the invariant $-CH(CH_3)_2$ cross peaks of Leu32 at −0.70, 0.29 ppm and −0.90, 0.29 ppm. For individual amino acids, the observed NH–Cα H exchange rate constant was obtained by fitting graphs of the cross-peak volume integrals against exchange time to a first-order exponential decay curve (Paterson et al., 1990). The protection factors were calculated as the ratios of exchange rate constant in free forms to those in complexed forms (k_{free}/k_{bound}).

Structural Modeling. Exchange protection factors and interprotein contacts within the 1:1 complex were color-coded as described in Results and Discussion and mapped onto the existing crystal structures of iso-1 cyt *c* (Berghuis & Brayer, 1992) and the 1:1 complex (Pelletier & Kraut, 1992) using coordinates deposited in the Protein Data Bank (Bernstein et al., 1977). Figures 5 and 6 were generated on a Silicon Graphics Iris 4D70 using the program INSIGHTII (Biosym).

RESULTS AND DISCUSSION

General Experimental Approach. The combination of hydrogen–deuterium exchange labeling and proton NMR has been recently used in protein complex studies (Paterson et al., 1990; McLendon, 1991). The fundamental basis for this method is that main-chain amide protons should exchange with deuterium so slowly as to allow a proton NMR experiment to detect specific individual, residual proton intensity after at least the shortest deuterium exposure time in the exchange

reaction. Previous data indicated that about 30%–40% of amide protons in cytochrome c satisfy this criterion for exchange carried out at pH 4.7–5.0 (Englander et al., 1984; Marmorino et al., 1993). In the work presented here the exchange was carried out at pH ~7.0, which is optimal for complex formation but is a pH where amide exchange is more rapid; consequently, we expected fewer protons to fulfill the exchange criterion than in those studies carried out at lower pH. In this work we classified fast, medium, and slow exchanging amide protons on the basis of our measured exchange rate constants for free yeast iso-1 ferricyt c. That is, an amide proton is classified as "fast" if k_{obs} is greater than 0.8 h^{-1}, "medium" if k_{obs} is between 0.8 and 0.1 h^{-1}, and "slow" if k_{obs} is less than 0.1 h^{-1}, and each residue in Table 1 is labeled with "f", "m", and "s" by these criteria. Among all the yeast iso-1 ferricyt c amide protons, only 24 displayed exchange rates at pH 7.0, 23 °C, that allowed NMR to monitor their exchange profiles as a function of time. This situation means that the binding site mapped by this technique may not be comprehensive.

Furthermore, although the time resolution of these H–D exchange experiments is consistent by virtue of the repetitive, identical protocol, it is "fuzzy" in the sense that it takes approximately 2 h between the time that the exchange reaction is quenched and the initiation of an NMR experiment. Although lowering both the pH′ (to 5.0) and the temperature (to 5 °C) at the end of the exchange time is done in order to suppress subsequent amide proton exchange, all subsequent exchange may not be completely eliminated. However, both the control iso-1 cyt c and iso-1 cyt c isolated from the CcP complex were treated identically in these experiments, and we expect that after the second column both free and CcP-bound cyt c behave identically so that the only experimental difference derives exclusively from the exchange period. So, the basic assumption for interpreting these experiments is that any experimentally observed perturbation of the amide exchange rate must be due to CcP binding during the exchange period. We conclude from our results that this method can successfully measure the differential exchange rates of 24 amide protons of iso-1 ferricytochrome c, due to CcP complexation.

We also wish to emphasize that we have studied the complex involving yeast iso-1 *ferri*cyt c, by subsequently studying the MCOSY spectrum of iso-1 *ferro*cyt c. Thus, the isotope exchange results we present and discuss below are specifically for the CcP/yeast iso-1 *ferri*cyt c. We have chosen the CcP/iso-1 ferricyt c complex as our first study for these reasons: (1) because the results would be relevant to prior NMR studies of CcP/ferricyt c complexes (Satterlee et al., 1987; Moench et al., 1992; Yi et al., 1992, 1993a, 1994); (2) because it is the so-called "product" complex in the proposed CcP enzymatic reaction sequence (Poulos & Kraut, 1980; Poulos & Finzel, 1984; Bosshard et al., 1991); (3) because it is one of the most stable complexes among all the possible 1:1 complexes between CcP and cytochrome c (Yi et al., 1993b) and stability over 6 days was required to complete these experiments; and (4) because yeast iso-1 cyt c in the complex crystal structure was in the ferric form (Pelletier & Kraut, 1992).

Proton Assignments of Native Yeast Iso-1 Ferrocyt c. The combination technique of H–D exchange labeling and proton NMR spectroscopy requires extensive knowledge of proton assignments of yeast iso-1 ferrocyt c, particularly in the NH–CαH cross-peak region (frequently referred to as the "fingerprint" region) of the homonuclear proton COSY spectrum. Unambiguous assignments are the basis for identifying specific

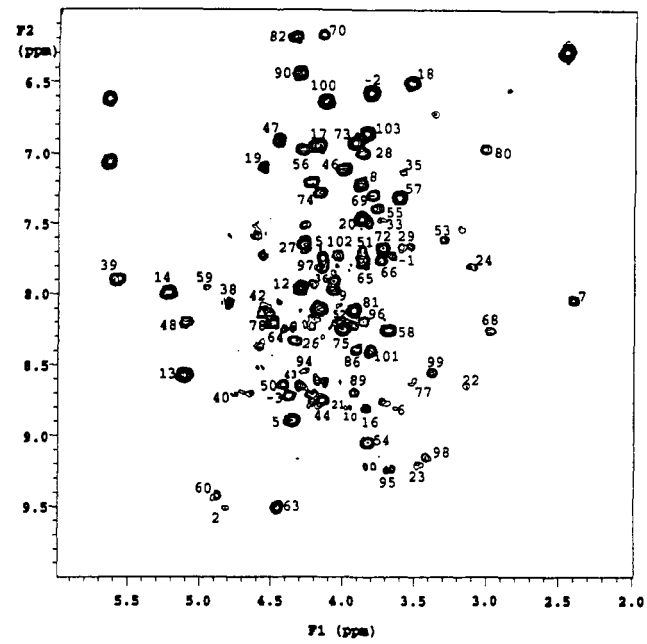

FIGURE 1: 500-MHz proton NMR contour plot of the fingerprint region of the homonuclear MCOSY spectrum of the yeast iso-1 ferrocyt c in 50 mM phosphate/90% H_2O/10% D_2O buffer, pH 5.2 at 25 °C. The identified NH–CαH cross peaks of amino acids are labeled with the primary sequence numbers of their parent amino acids.

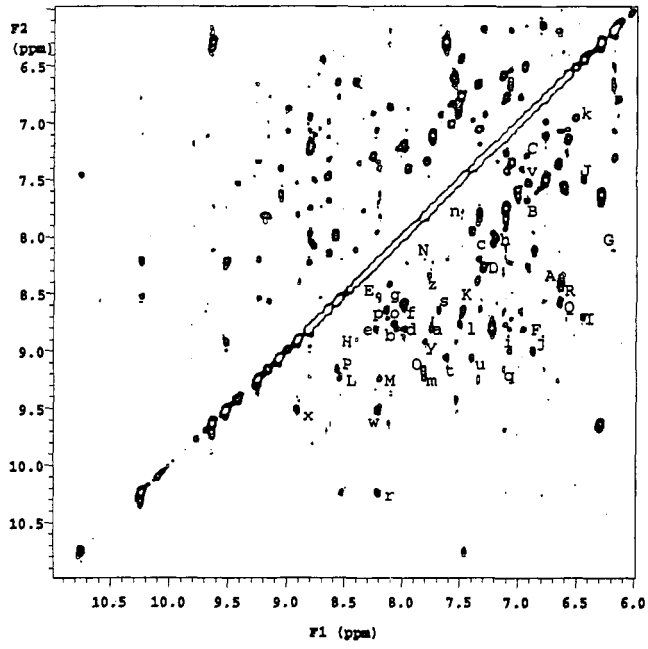

FIGURE 2: 500-MHz homonuclear proton NOESY contour plot of yeast iso-1 ferrocyt c (133-ms mixing time) showing the amide and aromatic region (50 mM phosphate/90% H_2O/10% D_2O buffer, pH 5.2 at 25 °C). Connectivities involving pairs of neighboring amide protons are labeled below the diagonal with letters of both upper and lower cases (a, 5–6; b, 6–7; c, 7–8; d, 9–10; e, 10–11; f, 12–13; g, 13–14; h, 14–15; i, 15–16; j, 16–17; k, 17–18; l, 20–21; m, 23–24; n, 32–33; o, 37–38; p, 40–41; q, 45–46; r, 48–49; s, 50–51; t, 53–54; u, 54–55; v, 55–56; w, 62–63; x, 63–64; y, 64–65; z, 66–67; A, 69–70; B, 72–73; C, 73–74; D, 74–75; E, 77–78; F, 79–80; G, 81–82; H, 86–87; I, 89–90; J, 90–91; K, 91–92; L, 94–95; M, 95–96; N, 96–97; O, 97–98; P, 98–99; Q, 99–100; R, 100–101).

residues protected by CcP binding. Complete proton resonance assignments for native yeast iso-1 cyt c have not been published so far, but a mutant, C102T, has been assigned to the extent of 90% of its protons by Gao and co-workers (Gao et al., 1990). We carried out initial MCOSY and DQF-COSY experiments under conditions similar to those reported for the

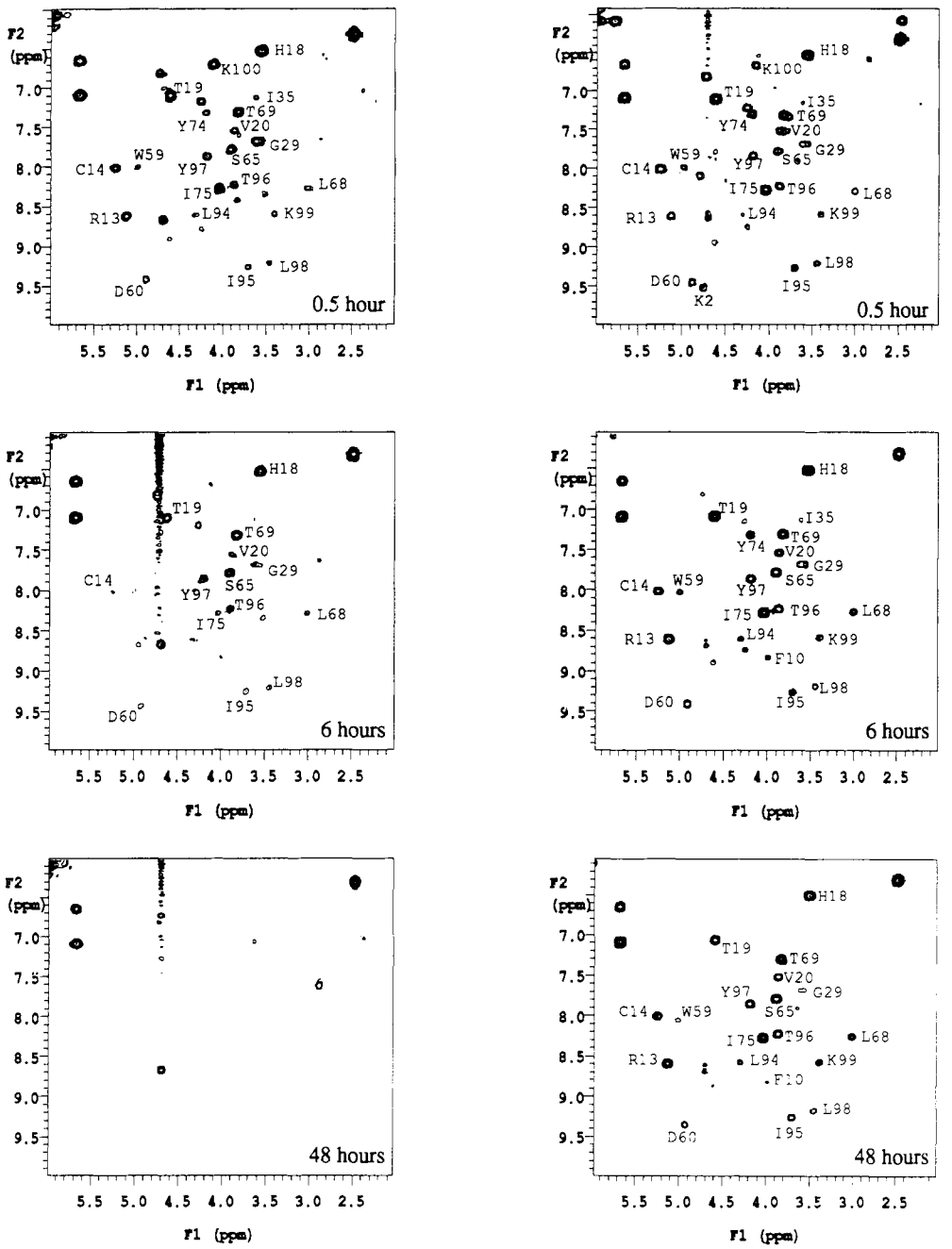

FIGURE 3: 500-MHz proton homonuclear MCOSY contour plots of fingerprint regions for representative cyt *c* samples after partial H–D exchange for free cyt *c* (left) and for CcP-bound cyt *c* (right). Data presented are for three exchange times which are labeled on the figures. The NH–CαH cross peaks of amino acids are labeled with their primary sequence number.

C102T mutant. Even though this C102T variant is claimed to be structurally identical to the wild-type protein (Gao et al., 1990, 1991; Berghuis & Brayer, 1992), and the overall pattern of cross peaks in the fingerprint region of their NMR spectra is very similar to that of wild-type iso-1 ferrocyt *c*, significant variations still exist. This meant we could not make straightforward use of the published C102T iso-1 cyt *c* proton assignments in this work without introducing unnecessary ambiguities. Consequently, we had to carry out a full suite of homonuclear proton COSY, DQF-COSY, TOCSY, and NOESY experiments for the wild-type iso-1 ferrocyt *c* in order to unambiguously assign as many proton resonances as possible, focusing primarily on the peptide main-chain CαH and NH resonances.

Figure 1 shows the fingerprint region of a wild-type yeast iso-1 ferrocyt *c* MCOSY spectrum that was collected under conditions similar to those of the C102T mutant and is plotted as identically as possible to Figure 2 of Gao et al. (1990). This experiment was used to locate the NH–CαH cross peaks and fostered initial guesses at assignments in the wild-type iso-1 ferrocyt *c* spectrum. Subsequently, NOESY spectra were examined in the amide region (Figure 2) to obtain main-chain sequential connectivities using the procedures described by Wuthrich (1986). Additional assignments including obvious β-, γ-, and δ-protons were obtained from COSY and TOCSY spectra (data not shown). The extensive assignments we have so far accomplished (Table 1) allowed unambiguous identification of individual NH–CαH cross peaks after hydrogen–deuterium exchange labeling.

Protection Factors. Figure 3 is a representative side-by-side comparison of contour plots of homonuclear proton MCOSY NH–CαH regions as a function of deuterium exchange time for both free and bound forms of yeast iso-1 cyt *c*. Shown in Figure 3 are some time progressions showing

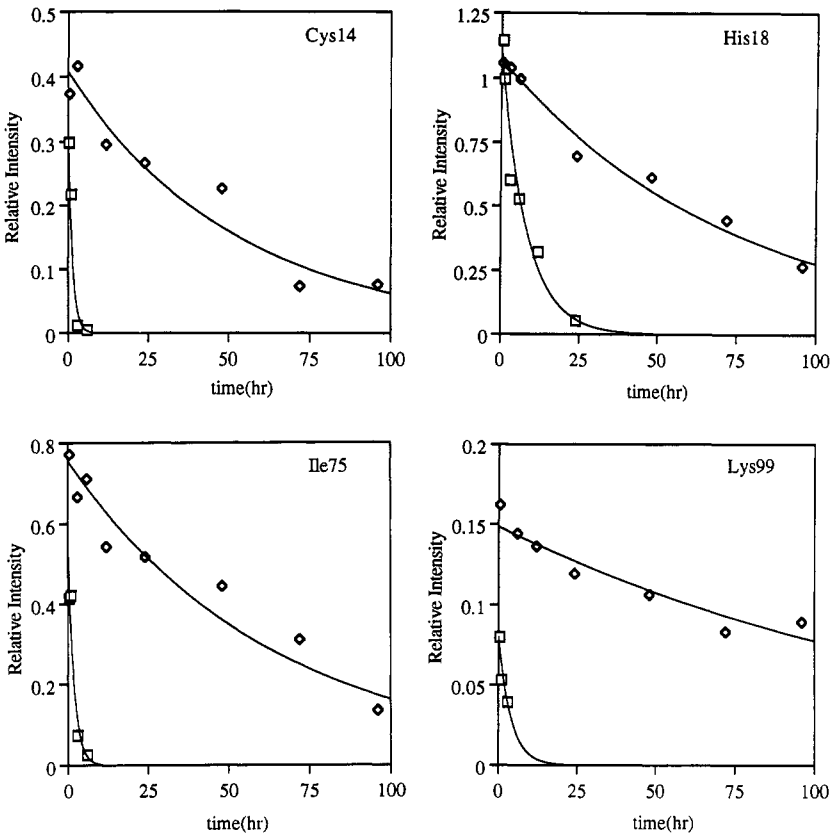

FIGURE 4: Hydrogen–deuterium exchange profiles for some of the iso-1 ferricyt c amide protons. Plotted are integrated cross-peak intensities against exchange time for free cyt c (squares) and CcP-bound cyt c (diamonds) in 10 mM KNO_3 solution, pH 6.5 at 23 °C. The curves were obtained by fitting the experimental data to a first-order exponential decay.

cross-peak intensity changes observed by proton MCOSY spectra of iso-1 ferrocyt c. It is clear from these parallel comparisons that iso-1 ferricyt c that was bound to CcP consistently displays higher peak intensities at longer exchange time than does iso-1 ferricyt c that was not bound to CcP. This observation held true through three repetitions of the exchange experiment. Thus, even from this qualitative analysis of the raw data, it is clear that CcP has protected specific amide protons on iso-1 ferricyt c from deuterium exchange. In order to quantitate the CcP protection effect, NH–CαH cross peaks in the iso-1 ferrocyt c MCOSY spectra were integrated for each of the exchange times. From these volume integrals, the observed H–D exchange rate constant of an individual amide proton was estimated by fitting graphs of the individual integrated intensities plotted against exchange time to a first order exponential decay (Paterson et al., 1990; Marmorino et al., 1993). Figure 4 shows some of these digitized data and their exponential fits. Numerical results are listed in Table 2.

Some iso-1 protection factors are found to be significant even though they are not as high as the factors of ~300 previously found in the antibody/horse cyt c complex (Paterson et al., 1990). However, they are much higher than the protection factors recently reported for horse ferricyt c in a similar complex (Jeng et al., 1994). For our purposes here and on the basis of three repetitions of these experiments, we consider it significant to reflect a protection factor of 8 or greater. The data presented here confirm that CcP and yeast iso-1 ferricyt c form a highly specific, tight-binding complex in low salt condition. The data presented in Table 2 reveal that strongly protected residues are generally located in the 10's helix, the 70's helix, residues 59 and 60, and the 90's helix. The protection pattern is represented by color-coding in Figures 5 and 6. In Figure 5 (view of the heme solvent-exposed edge), the amino acids with protection factors of 8 or greater, as determined in this work, are colored in blue whereas amino acids of iso-1 cyt c found to interact with CcP

Table 2: Observed Amide Proton H–D Exchange Rate Constants for Amino Acids in Yeast Iso-1 Ferricyt c Free in Solution and CcP Bound[a]

residue	H-bond partner	free (h^{-1})[b]	bound (h^{-1})[b]	protection factor[c]
Phe10		0.152 ± 0.100	0.017 ± 0.018	8.9
Arg13	Leu9	0.156 ± 0.118	0.012 ± 0.0056	13
Cys14	Phe10	0.384 ± 0.128	0.011 ± 0.0057	35
Cys17	Leu15	0.205	0.060	3.4
His18	Cys14	0.066 ± 0.018	0.004 ± 0.001	20
Thr19	H_2O	0.057 ± 0.0089	0.007 ± 0.002	8
Val20	H_2O	0.103 ± 0.0570	0.003 ± 0.001	30
Gly29	Cys17	0.216 ± 0.106	0.006 ± 0.002	40
Ile35	Leu32	0.063 ± 0.035	0.022 ± 0.014	2.9
Trp59	Arg38	0.183 ± 0.073	0.015 ± 0.011	12
Asp60		0.056 ± 0.044	0.002 ± 0.002	30
Ser65	Asn62	0.026 ± 0.0056	0.002 ± 0.001	10
Leu68	Glu66	0.032 ± 0.013	0.003 ± 0.002	10
Thr69	Ser65	0.040 ± 0.015	0.003 ± 0.002	10
Lys73	Pro71	0.178	0.016	11
Tyr74	Asn70	0.633 ± 0.0677	0.026 ± 0.013	24
Ile75	Pro71	0.167 ± 0.0524	0.006 ± 0.003	30
Leu94		0.128 ± 0.033	0.006 ± 0.002	20
Ile95	Arg91	0.069 ± 0.039	0.004 ± 0.002	20
Thr96	Asn92	0.038 ± 0.015	0.002 ± 0.002	20
Tyr97	Leu94	0.039 ± 0.021	0.002 ± 0.001	20
Leu98	Leu94	0.036 ± 0.025	0.004 ± 0.003	10
Lys99	Ile95	0.067 ± 0.038	0.002 ± 0.001	30
Lys100	Thr96	0.124 ± 0.128	0.014 ± 0.011	8.8

[a] In 10 mM KNO_3, pH′ 6.5 at 23 °C. [b] Error was estimated by t-test at 80% confidence level. For Cys17 and Lys73, the exchange rate constants were obtained from one trial out of three repeated runs so that there is no statistical error reported here. [c] The protection factor is the ratio of the H–D exchange rate constants: k_{free}/k_{bound}.

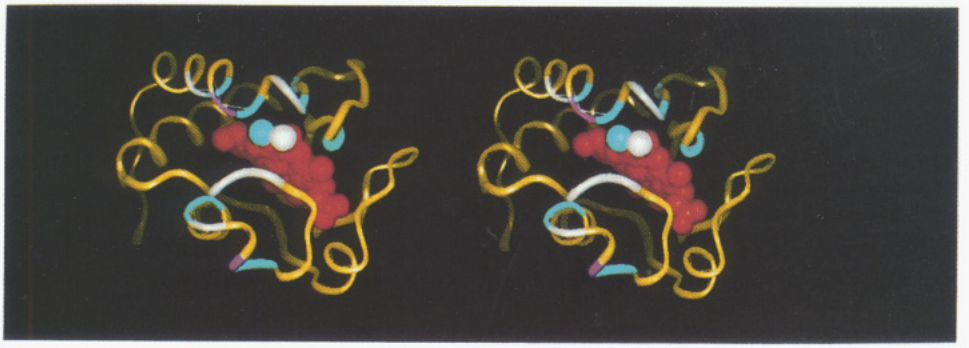

FIGURE 5: Computer graphics representation of the CcP binding site on yeast iso-1 ferricyt *c* based upon the published crystal structure of yeast iso-1 cyt *c* (Berghuis & Brayer, 1992). This view is of the heme solvent-exposed edge (the so-called front side). The protected regions determined by NMR and H–D exchange are colored in blue; the regions found to interact with CcP in the complex crystal structure (Pelletier & Kraut, 1992) are in white; the regions common to both studies are shown in purple. The ribbon backbone of iso-1 cyt *c* is shown in yellow, and the heme is in red. The heme 3-methyl substituent that exhibits a significant complex-induced resonance shift is also represented as a blue sphere.

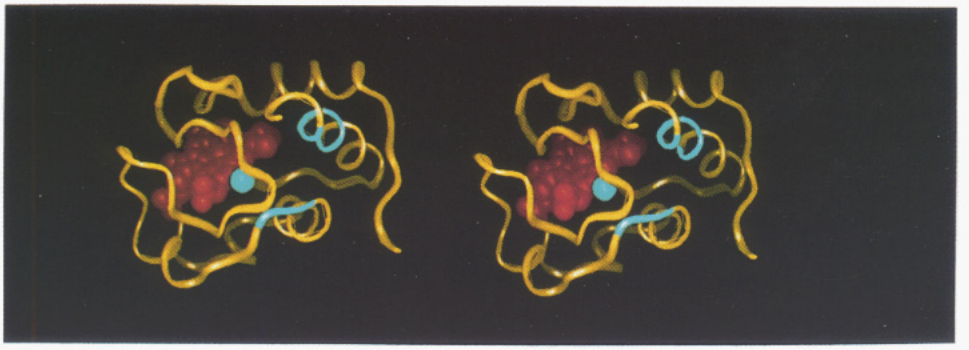

FIGURE 6: Computer graphics representation of the back side of yeast iso-1 ferricyt *c*. This is the opposite face of the molecule from the exposed heme edge shown in Figure 5. The regions found with elevated amide isotope exchange protection factors as determined in NMR and H–D exchange experiments are shown in blue. The ribbon backbone of iso-1 ferricyt *c* is shown in yellow. The heme is in red, and on the heme the 8-methyl substituent displaying a significant complex-induced resonance shift is also represented as a blue sphere.

in the crystal structure of the complex (Pelletier & Kraut, 1992) are shown in white. Residues common to both are colored in purple. The ribbon backbone of cyt *c* is shown in yellow, and the heme is in red. This figure shows that some of the regions exhibiting a high H–D protection effect are obviously compatible with the binding interface defined by the complex cocrystal structure (Pelletier & Kraut, 1992), while others are not.

CcP Primary Binding Site and Comparison with the Complex Crystal Structure. Although based on limited data, the most straightforward interpretation of the present results is that in solution the primary CcP binding site on yeast iso-1 ferricyt *c* includes part of the 10's and 70's helices. In fact, these two segments are in good agreement with the interaction site defined by the solid-state complex crystal structure of the CcP/yeast iso-1 ferricyt *c* complex (Pelletier & Kraut, 1992), as presented here in Figure 5 and Table 3. According to the complex crystal structure, the cytochrome *c* interaction domain consists of the following three discontinuous regions. Region 1 includes Leu9, Arg13, Gln16, Cys17, and the heme 4β-CH_3 (CBC methyl; Pelletier & Kraut, 1992) on pyrrole ring C, which are located above the heme solvent-exposed edge in Figure 5. Region 2 includes Ala81, Phe82, Gly83, and Lys87, which form a loop at the front of the heme solvent-exposed edge. Region 3 includes Asn70 and Lys73, at the bottom of the heme solvent-exposed edge. Consistent with this, our data show high protection factors in similar regions. These include Phe10, Arg13, Cys14, His18, Thr19, and Val20, which are close to heme pyrrole ring C and overlap with region 1, described above from the X-ray result. In addition, previous NMR studies (Moench et al., 1991, 1992; Yi et al., 1992, 1993a) have demonstrated that the proton resonance of the heme 3-CH_3 on pyrrole ring C displayed the largest complex-induced shift, which strongly implicated the ferricyt *c* heme pyrrole ring C in the protein–protein interface. Also, residues Leu68, Thr69, Tyr74, and Ile75, with high protection factors, describe the same region as Asn70 and Lys73, which compose region 3 of interaction in the complex crystal structure. So,

Table 3: Comparison of Yeast Iso-1 Ferricyt *c* Protected Amino Acid Residues Exhibiting CcP-Induced Protection in H–D Exchange Experiments with Those Residues in the CcP/Iso-1 Ferricyt *c* Interaction Interface Defined by Crystallography

H–D exchange reaction	CcP/yeast iso-1 ferricyt *c* cocrystal structure[a]	
iso-1 cyt *c*	iso-1 cyt *c*	CcP
Phe10	Leu9	Tyr39
Arg13	Arg13	Tyr39
Cys14		
heme 3-CH_3[b]	heme 4β-CH_3	Ala193 and Ala194
His18	Gln16	Ala193
Thr19	Cys17	Ala193
Val20		
Leu65		
Leu68		
Thr69	Asn70	Glu290
Lys73	Lys73	Glu290
Tyr74		
Ile75		
	Ala81	Val197
	Phe82	Val197
	Gly83	Val197 and Gln120
Trp59		
Asn60		
Leu94–Lys100		

[a] Pelletier & Kraut, 1992. [b] Identified by chemical shift perturbation in the complex (Yi et al., 1993).

Table 4: Chemical Shift Comparison for Proton Resonances of Yeast Iso-1 Ferricyt c Free in Solution and CcP Complexed

resonance	free (ppm)[a]	bound (ppm)[a]	difference[b] (Hz)
Pro30δ	−6.103	−5.394	354.5
Pro30δ′	−1.826	−1.621	102.5
Trp59ζ	7.409	8.050	320.5
Leu68δ	−3.586	−3.937	−175.5
Leu68δ′	−1.141	−1.324	−91.5

[a] The chemical shifts were obtained from 500-MHz one-dimensional proton NMR spectra and two-dimensional COSY and NOESY spectra in 10 mM KNO_3/D_2O, pH′ 6.5 at 20 °C. The residual H_2O resonance was used as reference at 4.70 ppm. [b] Difference = chemical shift (bound) − chemical shift (free). This is the complex-induced shift.

we conclude that the protection of the residues in the 10's helix and the 70's helix identified by H–D exchange labeling is compatible with the protein–protein interface found in the crystal structure.

From the comparison above, it is obvious that we could not detect any residues in the 80's primary sequence region of iso-1 cyt c, which was found in van der Waals contact with CcP in the crystal. The amide protons in this loop exchange extremely fast, probably due to the nature of structural flexibility of this region. Upon inspection of the topographic arrangement of the 10's and the 70's helices and the 80's loop on the protein surface, it is obvious that the 80's loop is "sandwiched" in between the 10's helix and the 70's helix on the protein surface and it is right next to the heme pyrrole ring C. This structural arrangement strongly implies that the 80's loop must be involved in the primary interface of the tightly bound complex if CcP interacts with residues in both the 10's and the 70's helices.

Although presenting a picture of consistency with the crystallographic results, the specific, protected residues in the 10's and 70's helices found in H–D exchange labeling do not identically match the predicted interaction residues in the complex crystal structure. Explanations for this may be as follows. First, those specific interacting residues predicted by crystallographic data exhibit deuterium exchange rates too fast to be detectable under our experimental conditions. Second, this slight difference among these specific residues suggests that a slightly different interfacial orientation of the protein partners in the complex may occur in solution compared to the crystal. In support of this idea, it was pointed out by previous NMR evidence (Yi et al., 1993a) that the heme 3-CH_3 on pyrrole ring C showed the largest complex-induced proton shift while the heme 4β-CH_3 in pyrrole ring C experienced a very small change even though the heme 4β-CH_3 was found to interact directly with CcP in the crystal structure.

Further evidence supporting the region on yeast iso-1 ferricyt c that we have identified here as a primary interface for the solution complex is proton chemical shift data for several amino acid resonances in this region. Table 4 lists chemical shift comparisons for these residues in both free and CcP-bound forms of iso-1 ferricyt c under the same conditions as for the exchange reaction. For instance, two δ-CH_3 groups of Leu68 are shifted to lower frequency by 91.5 and 175.5 Hz in the CcP/yeast iso-1 ferricyt c complex, indicating magnetic environmental changes around this region. This evidence further suggests the involvement of the primary sequence segment which includes Leu68 in the CcP binding site.

In addition, amide protons of Gly29 and Ser65 displayed substantial protection factors (Table 2). In the iso-1 crystal structure (Berghuis & Brayer, 1992), the amide protons of Gly29 and Thr69 form H-bonds respectively to the carbonyl groups of Cys17 and Ser65 so that it is reasonable to expect that protection on Cys17 and Thr69 will extend to Gly29 and Ser65, respectively, via this H-bonding interaction. Similarly, Pro30 is located next to Gly29, and although it has no amide proton, its two Cδ-protons exhibit substantial complex-induced shifts (Table 4), indicating that CcP binds close enough to perturb their magnetic environment.

Protection Factors in Other Regions of Yeast Iso-1 Ferricyt c. Our results show that in iso-1 ferricyt c Trp59, Asn60, and all the amino acids in the latter 90's helix display elevated amide isotope exchange protection factors. This result seems hard to understand in light of the X-ray structure of the complex which shows that they are grouped on the "back side" of the heme away from the crystallographically defined interaction surface, as pictured in Figure 6. Because slower H–D exchange behavior in the complex can arise from direct shielding in the interface, from a conformational change due to protein–protein interaction, or from complex-induced dynamics changes, this experimental result leads to at least two possible interpretations.

First, perhaps the interaction interface in solution includes this "back" region of iso-1 ferricyt c. Previous solution chemical shift evidence gathered for both CcP and CcPCN complexes involving several different species of ferricyt c has consistently shown significant complex-induced proton hyperfine resonance shifts for the ferricyt c heme 8-CH_3 (Satterlee et al., 1987; Moench et al., 1992; Yi et al., 1992, 1993a, 1994). The heme 8-CH_3 is a substituent in heme pyrrole ring A, which is located on this same back side of iso-1 ferricyt c as Trp59. Our new data presented in Table 4 reveals that the newly identified Trp59 CζH resonance also displays a highly significant 320-Hz complex-induced shift. There are several ways that apparent expansion beyond the crystallographically defined region of this protein–protein interface to other regions of iso-1 ferricyt c might occur. All of these possibilities involve dynamic fluctuations that would not have been detected in the crystal structure.

(i) Dynamic rotational reorientation or motion of iso-1 ferricyt c while it is complexed to CcP could take place. There is some evidence to support this based on cross-linking and NMR studies that have found multiple forms of iso-1 ferricyt c cross-linked to CcP (Moench et al., 1992, 1993). Additionally, this type of behavior was predicted by a Brownian dynamics simulation of CcP and horse cytochrome c (Northrup et al., 1988, 1992). Whether it actually occurs has yet to be unambiguously proven.

(ii) It might be that dynamic fluctuation of CcP results in transient envelopment of this back side on iso-1 ferricyt c or that the actual complex structure in solution more totally envelopes yeast iso-1 than is shown by the crystal structure (Pelletier & Kraut, 1992).

(iii) In solution, yeast iso-1 ferricyt c might also be able to associate with CcP using the back side as a secondary interaction interface. Several recent interpretations of experimental data have provided alternative models for CcP and cytochrome c binding, such as "substrate-assisted" kinetic mechanisms for the complex dissociation process (McLendon et al., 1993; Yi et al., 1994) and 1:2 CcP/cyt c complexes (Stemp & Hoffman, 1993). Perhaps iso-1/iso-1 interactions inherent in these proposed models involve the iso-1 ferricyt c back side.

Second, it might be that CcP binding induces a conformational change in yeast iso-1 ferricyt c so as to indirectly retard amide exchange rates in this region. A conformational change is not obvious by comparing the crystal structure of the CcP/yeast iso-1 ferricyt c noncovalent complex (Pelletier

& Kraut, 1992) with the crystal structure of free iso-1 ferricyt *c* (Berghuis & Brayer, 1992). No significant conformational change was observed by superimposing these two structures except for a small change in the Gln16 side chain (Pelletier & Kraut, 1992). However, this does not rule out a conformational change occurring in solution where there are no crystal packing forces. In fact, long-range effects of protein–protein binding were previously observed upon H–D exchange in two antibody/horse cyt *c* complexes (Mayne et al., 1992). In that case, as here, the binding effect of the cytochrome *c* partner appeared to spread beyond the area of direct contact between the two proteins. We recognize that any such conformational change could affect the amide proton exchange dynamics in the C-terminal helix.

SUMMARY

Using H–D isotope exchange labeling with proton NMR spectroscopy and complex-induced chemical shift changes, we have attempted to map out the CcP binding site on yeast iso-1 ferricytochrome *c* for the noncovalent complex formed in solution at low ionic strength (10 mM KNO_3). The primary binding region defined by these NMR experiments includes parts of the 10's and 70's helices around the exposed heme edge and is in agreement with the binding region defined crystallographically. In addition, the solution studies involving both chemical shift perturbation and isotope exchange protection have identified an anomalously protected region in yeast iso-1 that is located away from the crystallographically defined interface. It involves the iso-1 ferricyt *c* C-terminus and the region close to heme pyrrole ring A. Although there are several possible causes for this surprising result, it may also be due to the difference in experimental conditions between these solution experiments (10 mM KNO_3) and the crystallization conditions (150 mM KCl; Pelletier & Kraut, 1992).

These results have demonstrated that isotope exchange NMR experiments may be a viable technique for studying the interaction between the redox partners in a naturally occurring mitochondrial complex. However, this method has limitations and results such as ours should be judged in this context. In our view, the most serious limitation to this work is a result of the necessity to carry out the isotope exchange at a pH near neutral and at room temperature. These conditions are near to physiological, and in any event, viability of complex formation required these conditions. However, with these conditions amide exchange rates are much faster than at low pH and 5 °C. This means that fewer of the total number of amide protons in the molecule are detectable, in the case presented here just 24. So, the basis for conclusions is limited to about one-fourth to one-fifth of the total amino acids. Thus, what this method cannot give is information about the fast exchanging amide protons, and at least in principle, it is conceivable that we have only detected part of what could be a more general overall slowing of isotope exchange in yeast iso-1 ferricyt *c* as a result of complex formation. Although possible, this prospect seems unlikely to us on the basis of the detected complex-induced shift changes which fall exactly in the same regions in which we have observed H–D exchange protection. Therefore, the precise extent of the binding site in this complex may not be completely determined by this H–D exchange technique alone. Another limitation is the accuracy and reproducibility of measuring volume integrals, particularly those of small cross peaks. Although we have found similar relative trends among our 24 detected amide protons throughout three repetitions of the H–D exchange protocol, there is wide variability in some of the measured rate constants (Table 2). Consequently, it is our opinion that multiple sets of experiments should be performed.

With respect to the recently published report on the CcP/horse ferricyt *c* complex that appeared while this paper was being reviewed (Jeng et al., 1994), there are notable differences with the work published here. We briefly describe these. First, the maximum protection factor found for the iso-1 ferricyt *c* complex is much larger (40) than is the maximum factor in the horse ferricyt *c* complex (5.9). Second, overall there are more amino acids that show significant protection in the iso-1 ferricyt *c* complex, and the protection factors for iso-1 ferricyt *c* are uniformly larger than for the horse ferricyt *c* complex. Third, whereas the general pattern of protection factors in the two cytochromes is similar for amino acids in the 10 and 70's primary sequence positions, iso-1 ferricyt *c* shows significant protection factors in the C-terminal helix (residues 94–100). Significant protection in this region was not noted in the horse ferricyt *c* complex. These differences are consistent with the species-specific differences in these complexes that we have previously noted in other NMR parameters, such as complex-induced chemical shifts (Moench et al., 1992, 1993; Yi et al., 1992, 1993a,b) and chemical exchange dynamics (Moench et al., 1992; Yi et al., 1994).

REFERENCES

Bax, A., Freeman, R., & Morris, G. (1981) *J. Magn. Reson. 42*, 164–168.

Berghuis, A. B., & Brayer, G. D. (1992) *J. Mol. Biol. 223*, 959–976.

Bernstein, F. C., Koetzle, T. F., Williams, G. J. B., Meyer, E., Shimanouchi, T., & Tasumi, M. (1977) *J. Mol. Biol. 112*, 535–542.

Bosshard, H. R., Anni, H., & Yonetani, T. (1991) in *Peroxidases in Chemistry and Biology* (Everse, J., Everse, K., & Grisham, M. B., Eds.) Vol. 2, pp 51–83, CRC Press, Boca Raton, FL.

Chance, B. (1950) *Fed. Proc. 9*, 160.

Englander, S. W., & Kallenbach, N. R. (1984) *Q. Rev. Biophys. 16*, 521–655.

Erman, J. E., & Vitello, L. B. (1980) *J. Biol. Chem. 255*, 6224–6227.

Gao, Y., Boyd, J., Williams, R. J. P., & Pielak, G. J. (1990) *Biochemistry 29*, 6994–7003.

Gao, Y., Boyd, J., Pielak, G. J., & William, R. J. P. (1991) *Biochemistry 30*, 7033–7040.

Geren, L., Hahm, S., Durham, B., & Millett, F. (1991) *Biochemistry 30*, 9450–9457.

Gupta, R. K., & Yonetani, T. (1973) *Biochim. Biophys. Acta 292*, 502–508.

Hahm, S., Durham, B., & Millett, F. (1992) *Biochemistry 31*, 3472–3477.

Hazzard, J. T., Poulos, T. L., & Tollin, G. (1987) *Biochemistry 26*, 2836–2848.

Hazzard, J. T., McLendon, G., Cusanovich, M. A., Das, G., Sherman, F., & Tollin, G. (1988a) *Biochemistry 27*, 4445–4451.

Hazzard, J. T., Moench, S. J., Erman, J. E., Satterlee, J. D., & Tollin, G. (1988b) *Biochemistry 27*, 2002–2008.

Ho, P. S., Hoffman, B. M., Kang, C. H., & Margoliash, E. (1983) *J. Biol. Chem. 258*, 4356–4363.

Jeng, M. F., & Englander, S. W. (1992) *J. Mol. Biol. 221*, 1045–1061.

Jeng, M. F., Englander, S. W., Pardue, K., Rogalsky, J. S., & McLendon, G. (1994) *Struct. Biol. 1*, 234–238.

Kang, C. H., Ferguson-Miller, S., & Margoliash, E. (1977) *J. Biol. Chem. 252*, 919–926.

Kornblatt, J. A., & English, A. M. (1986) *Eur. J. Biochem. 155*, 505–511.

Kumar, A., Wagner, G., Ernst, R. R., & Wuthrich, K. (1981) *J. Am. Chem. Soc. 203*, 3654–3658.

Leonard, J. J., & Yonetani, T. (1973) *Biochemistry 12*, 1465–1468.
Margoliash, E., Ferguson-Miller, S., Kang, C. H., & Brautigan, D. L. (1976) *Fed. Proc. 35*, 2124–2130.
Marmorino, J. L., Auld, D. S., Netz, S. F., Doyle, D. F., Young, G. B., & Pielak, G. J. (1993) *Protein Sci. 2*, 1966–1974.
Martin, G. E., & Zektzer, A. S. (1988) *Two Dimensional NMR Methods for Establishing Molecular Connectivity*, VCH Publishers, New York, NY.
Mayne, L., Paterson, Y., Cerasoli, D., & Englander, S. W. (1992) *Biochemistry 31*, 10678–10685.
McLendon, G. (1991) *Struct. Bonding 75*, 159–174.
McLendon, G., Zhang, Q., Wallin, S. A., Miller, K. M., Billstone, V., Spears, K. G., & Hoffman, B. M. (1993) *J. Am. Chem. Soc. 115*, 3665–3669.
Mochan, E. (1970) *Biochim. Biophys. Acta 216*, 80–95.
Moench, S. J., Shi, T. M., & Satterlee, J. D. (1991) *J. Biol. Chem. 264*, 9923–9931.
Moench, S. J., Chroni, S., Lou, B. S., Erman, J. E., & Satterlee, J. D. (1992) *Biochemistry 31*, 3661–3670.
Moench, S. J., Erman, J. E., & Satterlee, J. D. (1993) *Int. J. Biochem. 25*, 1335–1342.
Nicholls, P. (1964) *Arch. Biochem. Biophys. 106*, 25–48.
Nicholls, P., & Mochan, E. (1971) *Biochem J. 121*, 55–67.
Northrup, S. H., & Thomasson, K. A. (1992) *FASEB J. 6*, A474.
Northrup, S. H., Boles, J. O., & Reynolds, C. L. (1988) *Science 241*, 67–70.
Otting, G., & Wuthrich, K. (1987) *J. Magn. Reson. 75*, 546–549.
Paterson, Y., Englander, S. W., & Roder, H. (1990) *Science 249*, 755–759.
Pelletier, H., & Kraut, J. (1992) *Science 258*, 1748–1755.
Piatini, U., Sorenson, O. W., & Ernst, R. R. (1982) *J. Am. Chem. Soc. 104*, 6800–6801.
Poulos, T. L., & Kraut, J. (1980) *J. Biol. Chem. 255*, 10322–10330.
Poulos, T. L., & Finzel, B. C. (1984) *Pept. Protein Rev. 4*, 115–171.
Satterlee, J. D., Moench, S. J., & Erman, J. E. (1987) *Biochim. Biophys. Acta 917*, 87–97.
States, D. J., Haberkorn, R. A., & Reuben, D. J. (1982) *J. Magn. Reson. 48*, 286–292.
Stemp, E. D. A., & Hoffman, B. D. (1993) *Biochemistry 32*, 10848–10865.
Vitello, L. B., & Erman, J. E. (1987) *Arch. Biochem. Biophys. 258*, 621–629.
Vitello, L. B., Huang, M., & Erman, J. E. (1990) *Biochemistry 29*, 4283–4288.
Waldmeyer, B., & Bosshard, H. R. (1985) *J. Biol. Chem. 260*, 5184–5190.
Wuthrich, K. (1986) *NMR of Proteins and Nucleic Acids*, Wiley, New York.
Yi, Q., Erman, J. E., & Satterlee, J. D. (1992) *J. Am. Chem. Soc. 114*, 7907–7909.
Yi, Q., Erman, J. E., & Satterlee, J. D. (1993a) *Biochemistry 32*, 10988–10994.
Yi, Q., Alam, S., Ge, Y., & Satterlee, J. D. (1993b) *Techniques in Protein Chemistry*, Vol. 4, pp 605–613, Academic Press, Inc., New York.
Yi, Q., Erman, J. E., & Satterlee, J. D. (1994) *J. Am. Chem. Soc. 116*, 1981–1987.
Yonetani, T., & Ray, G. (1966) *J. Biol. Chem. 241*, 700–706.
Zhou, J. S., & Hoffman, B. M. (1993) *J. Am. Chem. Soc. 115*, 11008–11009.